Selection of affinity peptides for interference-free detection of cholera toxin

Jong Min Lim, Nam Su Heo, Seo Yeong Oh, Myung Yi Ryu, Jeong Hyun Seo, Tae Jung Park, Yun Suk Huh, Jong Pil Park

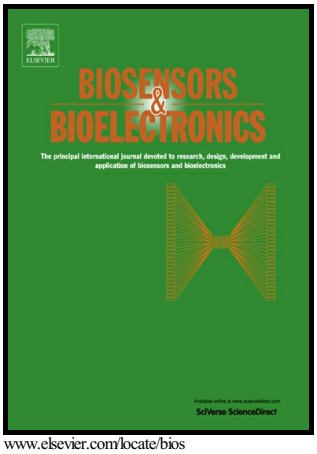

www.elsevier.com/locate/bios

PII: S0956-5663(17)30533-X
DOI: http://dx.doi.org/10.1016/j.bios.2017.07.075
Reference: BIOS9908

To appear in: *Biosensors and Bioelectronic*

Received date: 12 April 2017
Revised date: 28 July 2017
Accepted date: 30 July 2017

Cite this article as: Jong Min Lim, Nam Su Heo, Seo Yeong Oh, Myung Yi Ryu, Jeong Hyun Seo, Tae Jung Park, Yun Suk Huh and Jong Pil Park, Selection of affinity peptides for interference-free detection of cholera toxin, *Biosensors and Bioelectronic,* http://dx.doi.org/10.1016/j.bios.2017.07.075

Selection of affinity peptides for interference-free detection of cholera toxin

Jong Min Lim[11], Nam Su Heo[2,1], Seo Yeong Oh[2§], Myung Yi Ryu[1], Jeong Hyun Seo[3], Tae Jung Park[4], Yun Suk Huh[2*] and Jong Pil Park[1*]

[1]Department of Pharmaceutical Engineering, Daegu Haany University, Gyeongsan 38610, Republic of Korea

[2]Department of Chemical Engineering, Inha University, 100 Inha-ro, Nam-gu, Incheon 22212, Republic of Korea

[3]School of Chemical Engineering, Yeungnam University, Gyeongsan 38541, Republic of Korea

[4]Department of Chemistry, Chung-Ang University, 84 Heukseok-ro, Dongjak-gu, Seoul 06974, Republic of Korea

[1] These authors contributed equally to this work.

jppark@dhu.ac.kr (J.P. Park),

yunsuk.huh@inha.ac.kr (Y.S. Huh)

***** Corresponding author: Tel.: +82 53 819 1319, fax: +82 53 819 1406 (J.P. Park); Tel.: +82 32 860 9177, fax : +82 32 872 4046 (Y.S. Huh)

Abstract

Cholera toxin is a major virulent agent of *Vibrio cholerae*, and it can rapidly lead to severe dehydration, shock, causing death within hours without appropriate clinical treatments. In this study, we present a method wherein unique and short peptides that bind to cholera toxin subunit B (CTX-B) were selected through M13 phage display. Biopanning over recombinant CTX-B led to rapid screening of a unique peptide with an amino acid sequence of VQCRLGPPWCAK, and the phage-displayed peptides analyzed using ELISA, were found to show specific affinities towards CTX-B. To address the use of affinity peptides in development of the biosensor, sequences of newly selected peptides were modified and chemically synthesized to create a series of affinity peptides. Performance of the biosensor was studied using plasmonic-based optical techniques: localized surface plasmon resonance (LSPR) and surface-enhanced Raman scattering (SERS). The limit of detection (LOD) obtained by LSPR with 3σ-rule was 1.89 ng/mL, while SERS had a LOD of 3.51 pg/mL. In both cases, the sensitivity was much higher than the previously reported values, and our sensor system was specific towards actual CTX-B secreted from *V. cholera*, but not for CTX-AB_5.

Keywords: *Vibrio cholerae*; cholera toxin; phage display; affinity peptide; LSPR; SERS.

1. Introduction

Cholera is an acute intestinal infectious disease caused by the bacterium *Vibrio cholerae* (Espineira et al. 2010; Garrido-Maestu et al. 2015; Haddour et al. 2006; Jin et al. 2013). This bacterium can produce an endotoxin, cholera toxin (CTX), which can lead to severe dehydration and shock (Jin et al. 2013; Seo et al. 2012; Yamazaki et al. 2008). Therefore, CTX is considered as not only one of the major virulent factors of cholera, but also a common causative agent for diarrhea in humans (Cheng et al. 2004; Shirai et al. 1991). CTX has two subunits (Bunyakul et al. 2009; Kuramitz et al. 2011; Seo et al. 2012), A-subunit and B-subunit, which can assemble together into a hexametric arrangement of AB_5 family toxins. A-subunit (encoded by *ctxA* gene) is composed of two polypeptides responsible for the toxic activity, while B-subunit (encoded by *ctxB* gene) is a homo-pentameric, non-toxic subunit. It is responsible for specific binding of the toxin to GM1 ganglioside receptors on the surfaces of intestinal cells, and therefore, it is recognized as an adjuvant in the development of cholera vaccines for monitoring and controlling cholera outbreaks.

Conventional methods for CTX detection can be performed only after *V. cholerae* are isolated from the patients, which is a time-consuming and laborious approach (Jin et al. 2013; Shirai et al. 1991; Yamazaki et al. 2008). Thus, there has been increasing demand for development of new diagnostic techniques that are capable of simple, rapid, and inexpensive CTX detection. In recent years, tremendous analytical methods such as fluoro-immunoassay (Bunyakul et al. 2009; Haddour et al. 2006), microarray-based detection (Kim et al. 2012; Seo et al. 2012), colorimetric assay with polymers (Schofield et al. 2007), and nanoparticle-based multiplexing detection (Cheng et al. 2004; Connelly et al. 2012) have been proposed. For example, lactose-tethered gold nanoparticles or ganglioside GM1-tethered polymers can

achieve rapid and sensitive detection of CTX at concentrations as low as 0.2 pmol and 54 nmol, respectively (Kilian et al. 2007; Schofield et al. 2007). However, specific recognition of these methods is mainly based on either antibody, GM1, or both (Kuramitz et al. 2011). For point-of-care applications, development of new recognition agents over antibodies for early prediction and detection of cholera may be preferred.

Phage display is a powerful method that enables identification of new target-specific peptides in a short period of time (Hwang et al. 2015; Hwang et al., 2016, Hwang et al., 2017; Park et al. 2010; Park et al., 2015; Sidhu 2001; Wu et al. 2011). There are a number of successful examples of this approach: identification of GM1-specific binding peptides (Matsubara et al. 1999), identification of inorganic material-binding peptides (Gabryelczyk et al. 2013; Sarikaya et al. 2003; Sawada et al. 2013), and selection of unique peptides or proteins (Park et al. 2010; Sano et al. 2004; Wu et al. 2010). The advantages of using affinity peptides as recognition elements are their small sizes and cost-efficiencies in developing new bioassay systems (Hwang et al. 2015; Wu et al. 2011). More importantly, affinity peptides require less cost for manipulation, production, and show lower immunogenicity (Park et al. 2010).

Meanwhile, a number of bioanalytical detection platforms have been developed, which can be applied in clinical and biotechnological applications. Among various biosensing methods, localized surface plasmon resonance (LSPR) and surface enhanced Raman spectroscopy (SERS)-based bioanalytical techniques are frequently used for their rapid response, label-free detection, and reliability (Heo et al. 2016; Sepulveda et al. 2009). Thus, both methods can provide an ultrasensitive level of detection of desired targets (Chon et al. 2010; Huh and Erickson 2010).

In this study, we performed biopanning of M13 phage library to screen unique and short linear peptides that enable the recognition and detection of CTX-B. After several rounds of biopanning, CTX-B binding peptides were identified, chemically synthesized, and their binding affinity was characterized by using enzyme-linked immunosorbent assay (ELISA), LSPR, and SERS.

2. Materials and methods

2.1. Chemicals

Biotinylated cholera toxin subunit B, Tween 20, and 2,2′-azino-bis(3-ethylbenzothiazoline-6-sulfonic acid (ABTS) diammonium salt were purchased from Sigma-Aldrich (St. Louis, MO, USA). Horseradish peroxidase (HRP) conjugated anti-M13 monoclonal antibody was purchased from GE Healthcare (Piscataway, NJ, USA). Unless otherwise stated, all chemicals were of reagent grade. Gold (III) chloride trihydrate, sodium citrate dehydrate, 3-aminopropyl triethoxysilane (APTES), which was used as a linker of AuNPs, and glass film were purchased from Sigma-Aldrich. A glass film for a sensor chip was obtained from CARA Nano Glass Technology (Gumi, Korea). A series of synthetic peptides (CTX BP1-BP4) was chemically synthesized by Peptron (Daejeon, Korea). The secondary antibody of anti-mouse IgG labeled with Cy3 for SERS detection was purchased from GE Healthcare Life Sciences (Cy3 Ab Labeling Kit, Chicago, IL, USA).

2.2. Evolutionary screening of peptides (biopanning)

Biotinylated CTX-B was dissolved in 50 mM Tris-HCl (pH 7.0) and transferred to the

wells of 96-microwell plates. After overnight incubation at 4 °C with mild shaking, pre-immobilized wells were filled with blocking buffer (0.1 M $NaHCO_3$, pH 8.6), 5 mg/mL of bovine serum albumin (BSA), 0.02 % of NaN_3), and incubated at 4 °C for 1 h. After removing the unbound and residual blocking solution, wells were washed six times with TBST buffer (50 mM Tris–HCl, pH 7.5, 150 mM NaCl, 0.1% Tween 20). The Ph.D.-12 random peptide library (1.5×10^{13} pfu) was added to the pre-immobilized well, and the plate was shaken gently for 1 h at room temperature. To remove unbound phages, the plate was washed 10 times with TBST. Three rounds of biopanning were performed against CTX-B proteins. After washing, the bound phages were eluted using 100 µL of 0.2 M glycine-HCl (pH 2.2). The eluent was immediately neutralized with 15 µL of Tris-HCl (pH 9.1) to prevent destruction of the phages.

The eluted phages were amplified using *E. coli* ER2738 to make sufficient copies for subsequent rounds of biopanning. The amplified phages were harvested by NaCl/polyethylene glycol precipitation. After every round of biopanning, the recovered phages were titered by plating aliquots of the infected *E. coli* ER2738 prior to amplification on Luria–Bertani (LB) (BD Biosciences, San Jose, CA, USA) agar containing IPTG and X-gal.

2.3. ELISA for peptide binding to cholera toxin subunit B (CTX-B)

To evaluate whether the selected phage clones can specifically bind to CTX-B, ELISAs were performed. Plates were coated with biotinylated CTX-B for overnight incubation at 4 °C, blocked with blocking buffer, and washed six times with TBST solution. One hundred microliters of amplified phages (10^{11} pfu) were then added and incubated for 1 h at room

temperature. After washing six times with the same buffer to remove unbound phages, HRP-conjugated anti-M13 monoclonal antibody (diluted 1:10,000 in blocking buffer) was added and incubated at room temperature for 1 h. The antibody solution was removed, and the plate was washed again with TBST. Freshly prepared HRP substrates, ABTS were added and ELISA signal was measured at 405 nm using a microplate spectrophotometer (Multiskan FC, Thermo Scientific, Waltham, MA, USA).

2.4. Selection of the best peptides and optimization of concentration of peptides specific for CTX-B

To determine the best specific peptide against cholera toxin biomarker, CTX-B, 1 μg/mL each of a series of synthetic peptides, CTX BP1-BP4, was immobilized onto the LSPR substrates, washed three times with DI water, and incubated with varying concentrations of cholera toxin proteins. Finally, the absorbance signal was measured using a UV-vis spectrophotometer. In order to determine the optimal concentration between AuNPs and peptides, synthetic peptides (1 ng/mL to 100 μg/mL) capable of binding to CTX-B (1 pg/mL to 100 μg/mL) were reacted with AuNP-coated glass substrate at room temperature for 10 min. The optimization was performed by measuring change in the refractive index of the AuNP glass substrate modified with the peptides before and after reaction of cholera toxin proteins at a wavelength of 530 nm using a UV-vis spectrometer.

2.5. SERS detection performance

SERS analysis was also performed for more accurate detection of cholera toxin proteins. First, peptides (10 μg/mL) were reacted with the glass chip coated with AuNPs at room temperature for 10 min, followed by binding of CTX-B (10 μg/mL) to the peptide-conjugated

glass chip at room temperature for 10 min. After again washing the glass chip twice with DI water, 0, 0.01, 0.1, 1, 10, and 100 ng/mL of anti-mouse IgG labeled with Cy3 were added, respectively, and reacted with the glass chip at room temperature for 10 min. Finally, this dried sample was analyzed using a Raman spectrometer (UniRam, UniNanoTech) at a wavelength of 785 nm.

3. Results and discussion

3.1. Identification of novel peptides specific for cholera toxin subunit B (CTX-B) through phage display

We selected cholera toxin subunit B (CTX-B) as the target for identification of binding peptides using a phage display technique. To identify linear and unique binding peptides, we performed a biopanning of M13 phage library with a complexity of 4.3 x 10^{12} for CTX-B. The Ph.D.-12 random peptide library was added into pre-immobilized wells with biotinylated CTX-B, and the bound phages were eluted. After 3 rounds of biopanning, the peptides specific for CTX-B were identified. The yield after 3 rounds biopanning is shown in Tables S1 and S2. In most of the cases, 1 of 19 sequences was readable, indicating that a single dominant peptide was not found. However, these 6 peptide-displayed phage particles were chosen for further characterization: CTX-B R3#9 with amino acid VQCRLGPPWCAK, CTX-B R3#1 with amino acid SLLHTSMPSMIA, CTX-B R3#7 with DSQFNKYSIATV, CTX-B R3#17 with amino acid KVEPGTGAHSWQ, CTX-B R3#12 with amino acid VADSNWINPRGS, and CTX-B R3#13 with amino acid QGPHEHTKIHID. Since the sequence of CTX-B R3#7 showed up twice within the 19 clones that were sequenced; these

were also chosen for further characterization.

3.2. Sequence and secondary structural analysis of peptide-displayed phages

The final lead peptides have been very few charged amino acids (a single Arg and Lys) in peptide-displayed CTX-B R3#9 phages, and the sequences are rich in hydrophobic amino acids (Val, Leu, Pro, Trp, and Ala). It was suggested that hydrophobic interactions might be involved in the binding of the CTX-B. Each sequence contains a Cys, followed by Pro, which may induce a structural and/or flexible kink that is required for efficient binding of the targets.

3.3. Characterization of the selected phage clones for studying binding interactions

To evaluate the binding affinities of the selected phage clones for binding to CTX-B, ELISAs were performed. All 6 selected phage clones were tested, and the CTX-B R3#9 phage clones appeared to be the best, compared with other clones tested (Fig. 1A). As shown in Fig. 1, ELISA results showed that relative binding affinities of CTX-B R3#9 phages had a much higher than that of other phages, M13 wild type and BSA as a control. Therefore, we chose the CTX-B R3#9 phage clones as potential candidates for further characterizations.

3.4. Effects of cholera toxin subunit B concentrations on binding interactions

To further investigate the binding affinity at different CTX-B concentrations, CTX-B R3#9 peptides were incubated with pre-coated CTX-B (from 0.00086 to 5.1 μM), and the binding interactions were measured using ELISA. As shown in Fig. 1B, binding affinities of CTX-B R3#9 peptides gradually increased in a concentration-dependent manner. Interestingly, CTX-B R3#9 peptides showed specific binding for CTX-B at concentrations as low as 0.00086 μM. As expected, there is no comparable binding for BSA, indicating that CTX-B

R3#9 peptides bind specifically and selectively to their targets without non-specific binding.

3.5. Effects of phage concentrations on binding interactions

To evaluate binding affinities of the potential candidate clones, CTX-B R3#9 was bound to CTX-B at different concentrations of phages. CTX-B R3#9 clones at different concentrations ranging from 10^8 to 10^{11} pfu/mL were reacted with pre-immobilized CTX-B, and the binding interactions were measured from the ELISA signals. It was found that CTX-B R3#9 peptides exhibited increased binding affinity for CTX-B ranging from 10^9 to 10^{10} pfu/mL phage concentrations (Fig. 1C). However, the binding affinity did not increase at concentrations of 10^8 and 10^{11} phage particles. This is probably due to the loss of the avidity effect (Wu et al. 2011). Control experiments also showed the CTX-B R3#9 peptides had a higher affinity towards CTX-B than towards the wild-type M13 phage (data not shown).

3.6. Effects of serum on binding interactions

We tested the effects of serum on the binding properties of CTX-B. A total of 10^{10} pfu CTX-B R3#9 phages were incubated in TBS buffer with or without 1-10% of fresh fetal bovine serum (FBS) at room temperature for 1 h, and the binding affinity was measured using ELISA. Fig. 1D shows the binding affinity of the CTX-B R3#9 peptides to CTX-B in TBS with or without FBS. The binding affinities of phage clones were highly specific towards CTX-B, and they are not affected by the presence of 10% FBS.

To measure the binding constants of the selected peptides, we analyzed the CTX-B R3#9 phages by indirect ELISA assays. The apparent dissociation constants ($K_{d,app}$) showed nanomolar binding affinities for CTX-B (Fig. S1). Since dissociation constants for CTX-GM1 interaction have found to be 10^{-8}–10^{-12} M (Kuramitz et al. 2011; Schofield et al. 2007),

the binding affinities of the selected phages, CTX-B R3#9, are still comparable to those of CTX.

3.7. Synthesis and analysis of structural characteristics of affinity peptides

To apply the affinity peptide in the use of cholera toxin sensor, a series of cysteine-incorporated free peptides specific for CTX-B isolated from phage particles were chemically synthesized with high purity (>95%), as shown in Table S3. In detail, the CTX BP1 peptide has an amino acid sequence of VQCRLGPPWCAKGGGGSC, and we incorporated a cysteine residue (Cys) at the C-terminus for a thiol self-assembled monolayer and a linker (-GGGGS-) for molecular flexibility on the gold surface. In order to study the effects of amino acid composition on binding interactions, firstly, Val at position of 1, Leu at position of 5, Pro at positions of 7 and 8, Ala at position of 11, and Trp at position of 9 of the CTX BP1 were replaced by neutral and polar amino acids (like Gln, Ser, and Thr) to create the CTX BP2 peptide. Thus, they have an amino acid sequence of QQCRQGSSTCTKGGGGSC. Secondly, Arg at position of 4 and Lys at position of 12 of the CTX BP1 were replaced by polar and neutral amino acids (Ser and Thr, respectively) to create CTX BP3. Thirdly, Pro at positions of 7 and 8 of the CTX BP1 were replaced by Leu residues to create CTX BP4 to observe the effects of proline hinge and its molecular flexibility on the binding interaction (Table S2).

To study the effects of affinity peptide secondary structure on binding interactions, all synthesized affinity peptides were analyzed by circular dichroism (CD) spectroscopy. The molar ellipticity values of CTX BP1, CTX BP2, and CTX BP3 peptides were mostly similar, but not identical, random coil structures (Fig. S2 and S3).The analysis of CTX BP1 showed the following results: α-helix (6.4%), β-sheet (36.2%), and β-turn (14%), while the analysis

of CTX BP2 showed α-helix (3.7%), β-sheet (39.1%) and β-turn (14%). In case of CTX BP3, 6.7% of α-helix, 36.8% of β-sheet, and 14% of β-turn was observed. Unfortunately, a reliable spectrum could not be obtained with CTX BP4, possibly due to little salts or Cl^- ions in the samples. All three peptides can form a random coil structure. It is noteworthy that the CTX BP1 peptide was able to form a random coil structure, and it includes rich non-polar amino acids such as Val, Leu, Trp, and Ala, as well as two Pro residues. From these observations, we suggested that non-polar residues with a random coil structure and the Pro hinge are necessary for specific binding to CTX-B proteins.

3.8. Sensor operation and validation

In order to evaluate the selected CTX-B peptide for its use in a toxin biosensor, a series of peptides (CTB BP1~BP4) were chemically modified with a cysteine residue at the C-terminal for specific immobilization on a functionalized plasmonic substrate, and several experiments were performed by varying the concentrations of synthetic peptides (0.1, 1, and 10 μg/mL) to select the best peptides specific for CTX-B proteins. The screening of the peptides and preparation of the sensor included 3 steps: immobilization of the peptide, washing with buffer, and addition of CTX-B proteins. The change in absorbance was monitored by LSPR, as shown in Fig. 2. In detail, CTX-B proteins (1 μg/mL) were used in this experiment. LSPR results showed that immobilization of synthetic peptides resulted in increase in the absorbance (Fig. 2). Interestingly, a significant change in the absorbance was observed when CTB BP1 peptides were used (Fig. 2A). This indicates that specific binding of CTX-B protein with CTB BP1 peptides occurred on the plasmonic surface. However, no further significant difference in absorbance was observed when CTB BP2–4 peptides were immobilized, suggesting that binding affinities of these 3 peptides for CTX-B proteins were

not strong enough (Fig. 2B-D). Therefore, we selected CTB BP1 peptides as a potential candidate in the development of a toxin biosensor. We further explored the dynamic responses over a range of CTB BP1 peptide or CTX-B protein concentrations. After selection of the best peptides specific for CTX-B proteins, the concentration of CTB BP1 peptides was varied from 0.001–100 μg/mL with 10-fold serial dilution and reacted with the CTX-B proteins on a functionalized glass chip with gold nanoparticles. We found a quantitative response to a range of CTB BP1 peptide concentrations, indicating that it can be used as a toxin sensor in quantitative cholera toxin measurements (Fig. S4A). Based on these observations, we also tested the linear relationship of CTB BP1 peptides with a range of CTX-B protein concentrations. As expected, a quantitative change in the absorbance gradually increased with an increase in the concentration of CTX-B proteins from 0.00001 μg/mL to 100 μg/mL (Fig. S4B). The sensitivity obtained by LSPR with 3σ-rule was 0.01 ng/mL. This lower limit of detection is comparable to the detection of cholera toxin using ELISA and other assays (Ahn-Yoon et al. 2003; Jin et al. 2013; Kim et al. 2012). These results show that linear and unique peptides specific for cholera toxin exhibited femto-molar affinities for their target proteins, and they can thus be used in a new biosensor for the detection of cholera toxin.

To further quantify the dynamic range of detection for toxins, response curves over a range of secondary anti-cholera toxin B antibody tethered Cy3 concentrations in a sandwich assay format were monitored by LSPR, as shown in Fig. S4C. The reason why secondary antibody was used in LSPR measurements was to confirm that antibody can recognize and bind to CTX-B. Because our SERS probes were designed with Cy3 and antibody for highly sensitive detection of CTX-B. In detail, CTB BP1 peptides (10 μg/mL) and CTX-B proteins

(10 μg/mL) were sequentially reacted with the glass-gold chip. A quantitative response was monitored by varying the concentration of secondary Cy3-labeled antibody (0.0001-100 μg/mL). It is noted that there is a linear relationship between the change in absorbance and Cy3-labeled antibody concentration in the range from 0.00001 μg/mL to 100 μg/mL by both LSPR and SERS. In LSPR, the highest absorbance was observed at 100 μg/mL, which was considered as the saturation point (Fig. S4 A and B). In SERS, a good linear relationship was observed between CTB BP1 peptides and toxins (Fig. 3B). The LOD obtained by LSPR and SERS with 3σ-rule was 1.89 ng/mL and 3.51 pg/mL, respectively (Fig. S4C and Fig. 3A). There was a difference of LODs between LSPR and SERS. LSPR signal is dependent on the quantity of analytes bound to LSPR sensor layer and refractive index of the bound molecules, while SERS signal is based on the Raman signal that Raman active molecules can adsorb on the metal surface and tremendously increase in Raman signal up to 10^{14} (Chon et al. 2010; Huh and Erickson 2010). Form these observations, SERS may preferable to provide an ultrasensitive detection in our case. Thus, we confirmed that CTB BP1 peptides were much higher specific to cholera toxin the previously reported values (LOD), as shown in Table 1. Thus, it was concluded that this sensor system was selective for cholera toxin in the development of a toxin biosensor.

To illustrate feasibility of the sensor in a biological matrix, LSPR absorbance signal was recorded by varying the concentrations of bacterial culture supernatants with serial dilution. First, based on the results from the quantitative response with pure proteins of CTX-B, the feasibility of the detection was monitored by spiking CTX-B (100 pg/mL to 100 μg/mL) into bacterial LB media. As shown in Fig. 4, the absorbance of LSPR increased linearly with increasing concentration of spiked CTX-B, and the results showed high relationship between

the wide concentration range of CTX-B and absorbance signal (R^2 = 0.98) (Fig. 4A and 4B). In addition, the detection limit was found to be 1.89 ng/mL, which is quite acceptable for clinical test in patients. To further validate the sensor, another real bacteria (*V. parahaemolyticus*) as a negative control and bacterial culture broth containing toxin proteins were applied on the sensor without any further sample preparation (Fig. 4C and 4D). As expected, no quantitative intensities were observed for the negative samples, suggesting that this sensor system can be used in the development of new toxin sensor for highly specific and interference-free detection of the cholera toxin. Since this approach will require further characterization for clinical use, unstructured and linear affinity peptides used in this approach have several advantages compared to other detection methods. The affinity peptides as alternative biorecognition reagent over antibodies can be easily selected in short time and are cost-effective for mass production (Hwang et al., 2015, 2017; Wu et al., 2011).

Next, we tested the binding specificity of the sensor with whole cholera toxin (CTX-AB_5 complex) using various concentrations (1 pg/mL to 100 ng/mL). Whole cholera toxin consists of a single A and five B subunits. The complexation of A and B subunit to form AB_5 can affect binding affinity. Thus, it is necessary to test the performance of sensor using both toxin B and AB_5 complex. Interestingly, we found that no dynamic response was observed with increasing concentration of whole cholera toxin, indicating that the CTB BP1 affinity peptide does not bind to CTX-AB_5 which is a complexed form with A and B subunit. As shown in Fig. 4E and F, the absorbance signal of LSPR (Fig. 4E) and intensity of SERS (Fig. 4F) was not linearly correlated with target concentrations, indicating that the developed cholera toxin sensor can use for specific detection of the real cholera toxin.

4. Conclusion

In summary, unique and short peptides specific for cholera toxin subunit B (CTX-B) were identified from biopanning of M13 phage display peptide library, and the binding interactions of the peptide-displayed phage clones and a series of synthetic peptides were measured using ELISA, LSPR, and SERS. The peptide-displayed CTX-B R3#9 clones were chosen for the best peptides specific for binding to CTX-B. They had an amino acid sequence of VQCRLGPPWCAK. Using an indirect ELISA assay, the apparent dissociation constant ($K_{d,app}$) was found to have nanomolar affinity (6.7 nM).

Both LSPR and SERS results showed a quantitative response to a range of cholera toxin B concentrations. LOD obtained by with 3σ-rule in LSPR was 1.89 ng/mL, while SERS had a LOD of 3.51 pg/mL. It is noteworthy that the LODs are quite below the physiological concentration of cholera toxin in patient. Although both LSPR and SERS can produce lower LODs, SERS technique is preferable for highly specific detection of actual cholera toxin. To the best our knowledge, this is the first example of identification and evaluation of affinity synthetic peptides specific for CTX-B screened by M13 phage display technique. Since evolutionary phage display and plasmonic biosensor are mature techniques, and this general approach to cholera toxin sensor development is straightforward and can be applied for label- and interference-free detection of cholera toxin, as well as for providing a basis for monitoring and controlling cholera.

Acknowledgments

This study of JPP was supported by the National Research Foundation of Korea (NRF) grant funded by the Korea government (MSIP) (NRF-2014R1A2A2A01005621, NRF-2017R1A2A2A05001037). Moreover, this research of YSH was also supported by a grant

(17162MFDS065) from Ministry of Food and Drug Safety in 2017.

References

Adhikari, M., Dhamane, S., Hagstrom, A.E., Garvey, G., Chen, W.H., Kourentzi, K., Strych, U., Willson, R.C., 2013. Analyst 138, 5584–5587.

Ahn-Yoon, S., DeCory, T.R., Baeumner, A.J., Durst, R.A., 2003. Anal. Chem. 75, 2256–2261.

Archibald, M.M., Rizal, B., Connolly, T., Burns, M.J., Naughton, M.J., Chiles, T.C., 2015. Biosens. Bioelectron. 74, 406–410.

Bruzas, I., Unser, S., Yazdi, S., Ringe, E., Sagle, L., 2016. Anal. Chem. 88, 7968–7974.

Bunyakul, N., Edwards, K., Promptmas, C., Baeumner, A., 2009. Anal. Bioanal. Chem. 393, 177–186.

Cheng, Q., Zhu, S., Song, J., Zhang, N., 2004. Analyst 129, 309–314.

Chiriaco, M. S., Primiceri, E., D'Amone, E., Ionescu, R. E., Rinaldi, R., Maruccio, G., 2011. Lab Chip. 11, 658–663.

Chon, H., Lim, C., Ha, S.-M., Ahn, Y., Lee, E.K., Chang, S.-I., Seong, G.H., Choo, J., 2010. Anal. Chem. 82, 5290–5295.

Chung, W.J., Lee, D.Y., Yoo, S.Y., 2014. Int. J. Nanomedicine. 9, 5825–5836.

Connelly, J., Kondapalli, S., Skoupi, M., Parker, J.L., Kirby, B., Baeumner, A., 2012. Anal. Bioanal. Chem. 402, 315–323.

Espineira, M., Atanassova, M., Vieites, J.M., Santaclara, F.J., 2010. Food Microbiol. 27, 122–131.

Gabryelczyk, B., Szilvay, G.R., Salomaki, M., Laaksonen, P., Linder, M.B., 2013. Colloid.

Surface. B. 110, 66–73.

Garrido-Maestu, A., Chapela, M.-J., Vieites, J.M., Cabado, A.G., 2015. Food Microbiol. 46, 535–540.

Haddour, N., Chauvin, J., Gondran, C., Cosnier, S., 2006. J. Am. Chem. Soc. 128, 9693–9698.

Heo, N.S., Kwak, C.H., Lee, H., Kim, D., Lee, S., Kim, G.-b., Kwon, S., Kim, W.S., Huh, Y.S., 2016. J. Cryst. Growth. http://dx.doi.org/10.1016/j.jcrysgro.2016.09.039

Huh, Y.S., Erickson, D., 2010. Biosens. Bioelectron. 25 1240–1243.

Hwang, H.J., Ryu, M.Y., Lee, G.B., Park, J.P., 2016. ChemistrySelect. 1, 1140–1143.

Hwang, H.J., Ryu, M.Y., Park, C.Y., Ahn, J., Park, H.G., Choi, C., Ha, S.-D., Park, T.J., Park, J.P., 2017. Biosens. Bioelectron. 87, 164–170.

Hwang, H.J., Ryu, M.Y., Park, J.P., 2015. RSC Adv. 5, 55300–55302.

Jin, D., Luo, Y., Zheng, M., Li, H., Zhang, J., Stampfl, M., Xu, X., Ding, G., Zhang, Y., Tang, Y.-W., 2013. J. Clin. Microbiol. 51, 3968–3974.

Khemthongcharoen, N., Wonglumsom, W., Suppat, A., Jaruwongrungsee, K., Tuantranont, A., Promptmas, C., 2015. Biosens. Bioelectron. 63, 347–353.

Kilian, K.A., Bocking, T., Gaus, K., King-Lacroix, J., Gal, M., Gooding, J.J., 2007. Chem. Commun. 19, 1936–1938.

Kuramitz, H., Miyagaki, S., Ueno, E., Hata, N., Taguchi, S., Sugawara, K., 2011. Analyst. 136, 2373–2378.

Loyprasert, S., Hedstrom, M., Thavarungkul, P., Kanatharana, P., Mattiasson, B., 2010. Biosens. Bioelectron. 25, 1977–1983.

Matsubara, T., Ishikawa, D., Taki, T., Okahata, Y., Sato, T., 1999. FEBS Lett. 456, 253–256.

Park, J.P., Cropek, D.M., Banta, S., 2010. Biotechnol. Bioeng. 105, 678–686.

Park, J.P., Park, C.Y., Park, A.Y., Ryu, M.Y., 2015. RSC Adv. 5, 90531–90533.

Sano, D., Matsuo, T., Omura, T., 2004. Appl. Environ. Microbiol. 70, 3434–3442.

Sarikaya, M., Tamerler, C., Jen, A.K., Schulten, K., Baneyx, F., 2003. Nat. Mater. 2, 577–585.

Sawada, T., Okeya, Y., Hashizume, M., Serizawa, T., 2013. Chem. Commun. 49, 5088–5090.

Schofield, C.L., Field, R.A., Russell, D.A., 2007. Anal. Chem. 79, 1356–1361.

Schmit, V., Martoglio, R., Carron, K., 2012. Anal. Chem. 84, 4233–4236.

Seo, J.H., Lee, H.Y., Cha, H.J., 2012. Analyst. 137, 2860–2865.

Sepulveda, B., Angelome, P.C., Lechuga, L.M., Liz-Marzan, L.M., 2009. Nano Today. 4, 244–251.

Shirai, H., Nishibuchi, M., Ramamurthy, T., Bhattacharya, S.K., Pal, S.C., Takeda, Y., 1991. J. Clin. Microbiol. 29, 2517–2521.

Sidhu, S.S., 2001. Biomol. Eng. 18, 57–63.

Wu, J., Cropek, D.M., West, A.C., Banta, S., 2010. Anal. Chem. 82, 8235–8243.

Wu, J., Park, J.P., Dooley, K., Cropek, D.M., West, A.C., Banta, S., 2011. PLoS One. 6, e24948.

Yamazaki, W., Seto, K., Taguchi, M., Ishibashi, M., Inoue, K., 2008. BMC Microbiol. 8, 94.

Figure legends

Fig. 1. Characterization of selected peptide-displayed phage clones by ELISA. A) Relative binding affinity of identified phage-displayed peptides. B) Relative binding affinity of selected phage-displayed peptides at different CTX-B concentrations. C) Relative binding affinity of selected phage-display peptides. D) Effects of serum on binding interactions. All measurements were performed in triplicate and error bars represent standard deviations.

Fig. 2. Sensor preparation. Varying concentrations of peptides (1 mg/mL) in PBS buffer were immobilized on LSPR substrate and cholera toxin proteins (1 μg/mL) were introduced on pre-immobilized substrate, and the change in absorbance was measured before and after introduction of the target protein. All measurements were performed in triplicate and error bars represent standard deviations.

Fig. 3. Sensor preparation. A) SERS signal of CTX-B antibody-Cy3 at 1603 cm^{-1}, 1464 cm^{-1}, and 1445 cm^{-1}, and B) Dynamic linearity of SERS intensity at 1603 cm^{-1}.

Fig. 4. Specific detection of real biological cholera toxin produced from bacterial culture. A) LSPR spectra in the presence of the *V. cholera* O1 culture broth as positive with various concentrations. B) Dynamic response in change of LSPR absorbance with *V. cholera* O1 culture broth at 532 nm. C) LSPR spectra in the presence of the *V. parahaemolyticus* as negative sample. D) Dynamic response in change of LSPR absorbance with *V. parahaemolyticus* culture broth at 532 nm. E) LSPR intensity for CTX-AB_5 complexes with the sensor at 532 nm. F) SERS intensity of concentrations of CTX-AB_5 complexes.

Table 1. Comparison of the limit of detection (LOD) for detection of cholera toxin

Detection method	Target/Analyte	LOD	Reference
Colorimetric assay	cholera toxin B	3 μg/mL	(Schofield et al. 2007)
Optical detection	cholera toxin B	0.2 pM	(Kilian et al. 2007)
Electrochemical immunosensor	cholera toxin B	2 ng/mL	(Archibald et al. 2015)
Fluorescence immunoassay	whole cholera toxin	2 ng/mL	(Kim et al. 2012)
Immunoassay	whole cholera toxin	0.09 aM	(Loyprasert et al. 2010)
DNA sensor	*ctxA* gene	14 nM	(Khemthongcharoen et al. 2015)
Raman immunoassay	cholera toxin B	1100 ng/mL	Schmit et al. 2012
Gold nanodisk array with LSPR	cholera toxin B	20 nM	Bruzas et al. 2016
Flow immunoassay with EIS	cholera toxin B	1 ng/mL	Chiriaco et al. 2011
Affinity peptide-based assay	cholera toxin B	3.51 pg/mL	This study

Highlights

- A sensitive and interference-free plasmonic-based peptide sensor was developed.
- The detection performance for cholera toxin was monitored by LSPR and SERS.
- The limit of detection obtained by LSPR was 1.89 ng/mL, while SERS had 3.51 pg/mL.

fig 1

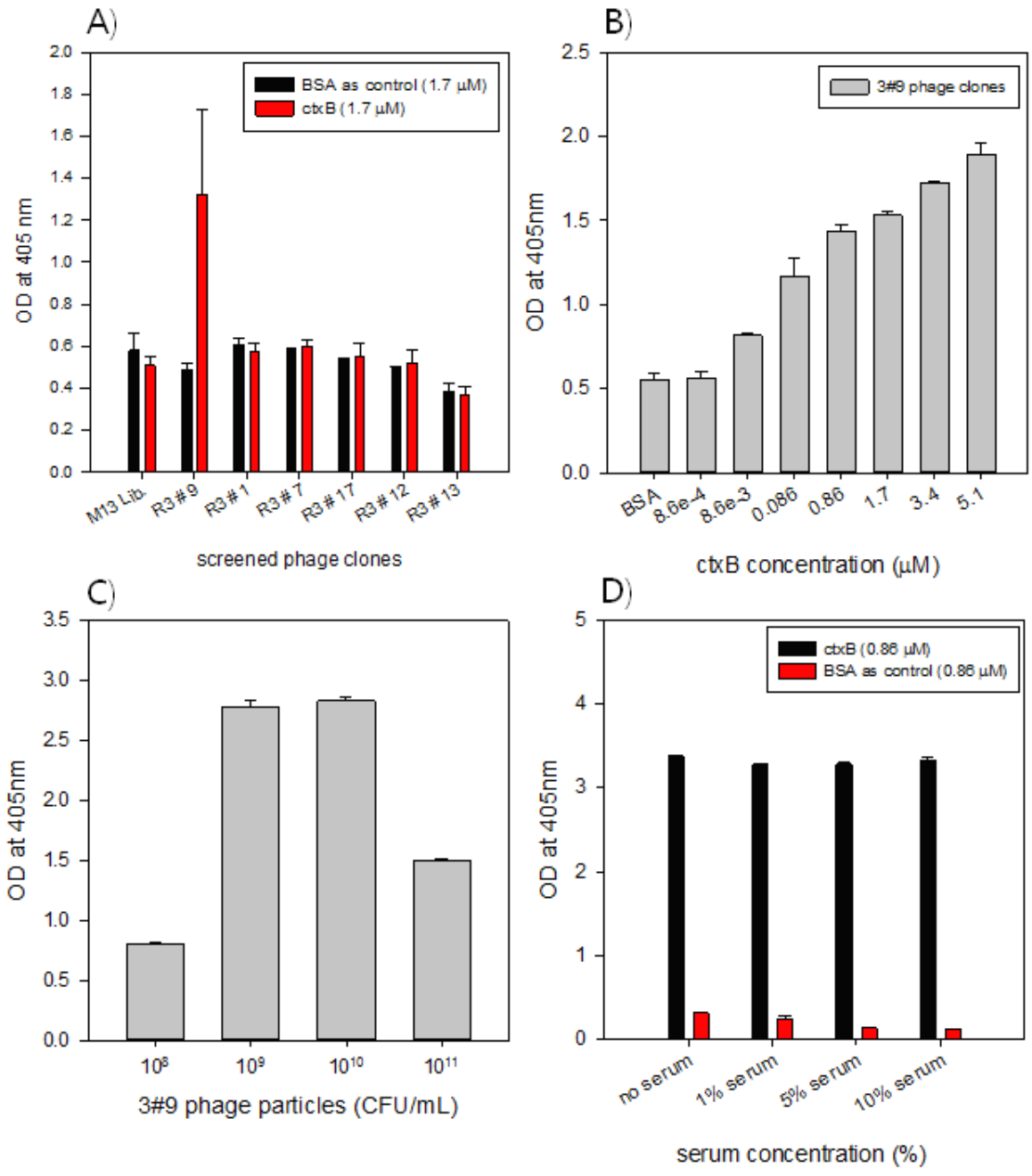
A)
BSA as control (1.7 μM)
ctxB (1.7 μM)
OD at 405 nm
M13 Lib.
R3#9
R3#1
R3#7
R3#17
R3#12
R3#13
screened phage clones
B)
3#9 phage clones
OD at 405nm
BSA
8.6e-4
8.6e-3
0.086
0.86
1.7
3.4
5.1
ctxB concentration (μM)
C)
OD at 405nm
3#9 phage particles (CFU/mL)
D)
ctxB (0.86 μM)
BSA as control (0.86 μM)
OD at 405nm
no serum
1% serum
5% serum
10% serum
serum concentration (%)

fig 2

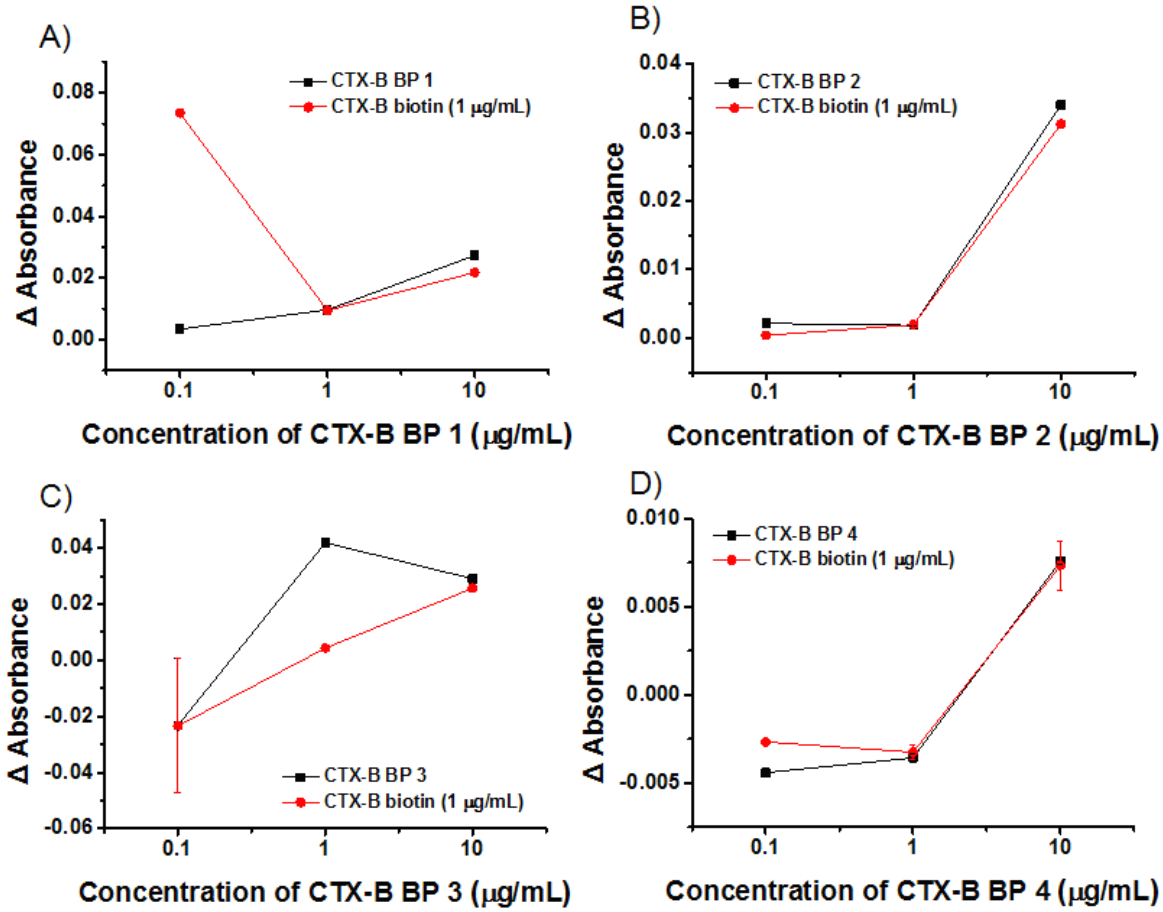
A)
CTX-B BP 1
CTX-B biotin (1 μg/mL)
Δ Absorbance
0.08
0.06
0.04
0.02
0.00
0.1
1
10
Concentration of CTX-B BP 1 (μg/mL)
B)
CTX-B BP 2
CTX-B biotin (1 μg/mL)
Δ Absorbance
0.04
0.03
0.02
0.01
0.00
0.1
1
10
Concentration of CTX-B BP 2 (μg/mL)
C)
CTX-B BP 3
CTX-B biotin (1 μg/mL)
Δ Absorbance
0.04
0.02
0.00
-0.02
-0.04
-0.06
0.1
1
10
Concentration of CTX-B BP 3 (μg/mL)
D)
CTX-B BP 4
CTX-B biotin (1 μg/mL)
Δ Absorbance
0.010
0.005
0.000
-0.005
0.1
1
10
Concentration of CTX-B BP 4 (μg/mL)

fig 3

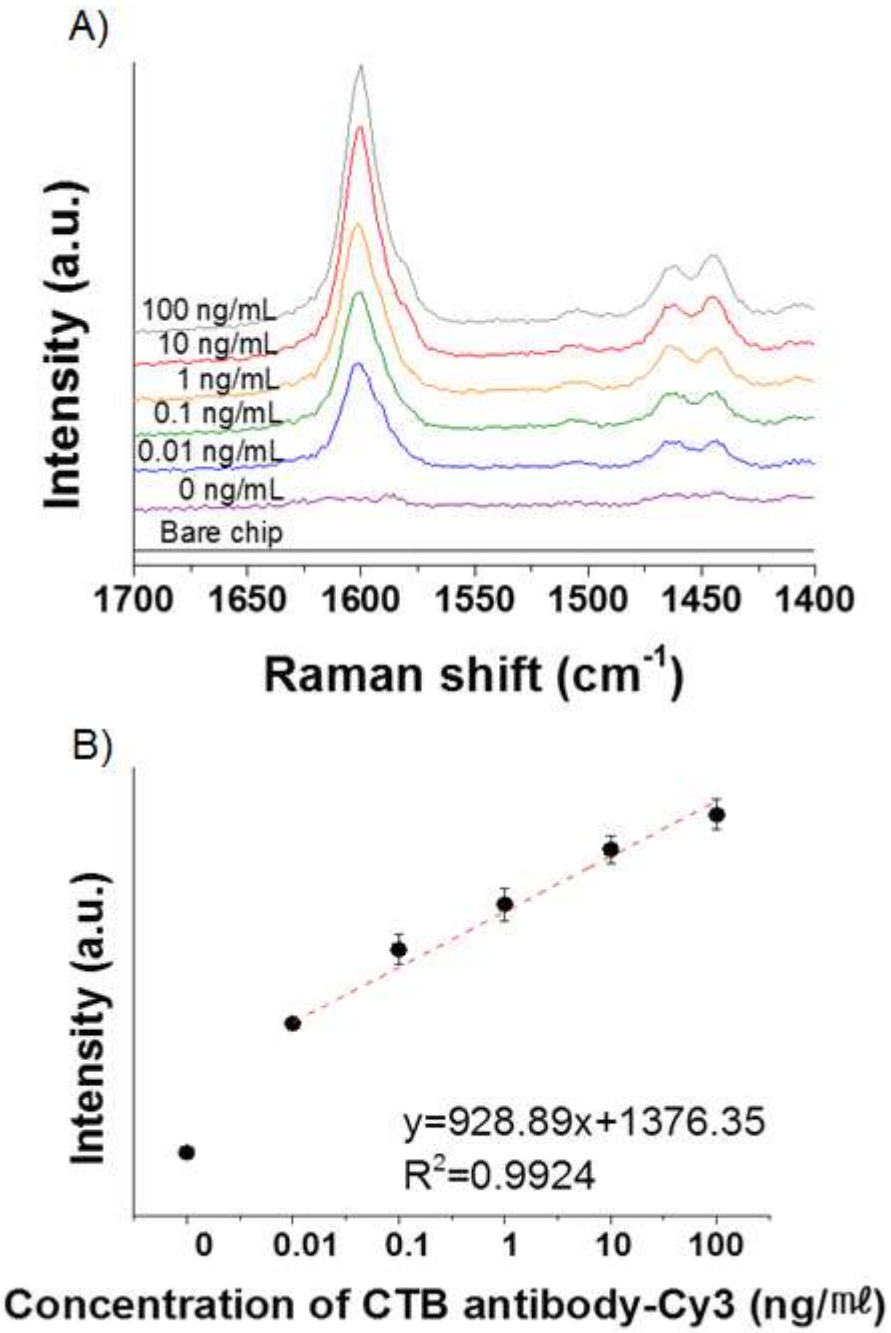
A)
Intensity (a.u.)
100 ng/mL
10 ng/mL
1 ng/mL
0.1 ng/mL
0.01 ng/mL
0 ng/mL
Bare chip
1700
1650
1600
1550
1500
1450
1400
Raman shift (cm-1)
B)
Intensity (a.u.)
y=928.89x+1376.35
R2=0.9924
0
0.01
0.1
1
10
100
Concentration of CTB antibody-Cy3 (ng/㎖)

fig 4

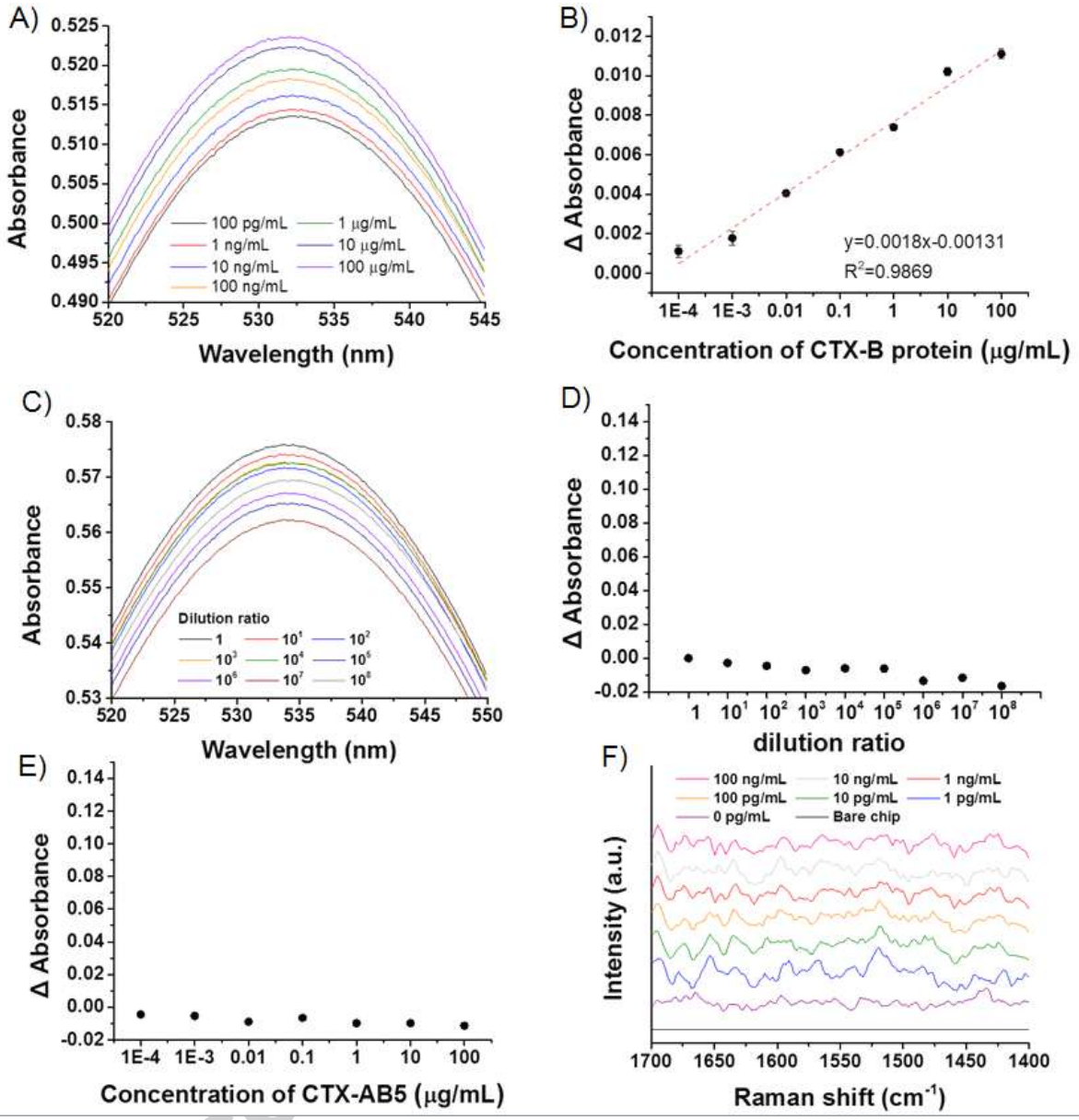
A)
Absorbance
Wavelength (nm)
100 pg/mL
1 ng/mL
10 ng/mL
100 ng/mL
1 μg/mL
10 μg/mL
100 μg/mL
B)
Δ Absorbance
Concentration of CTX-B protein (μg/mL)
y=0.0018x-0.00131
R²=0.9869
C)
Absorbance
Wavelength (nm)
Dilution ratio
D)
Δ Absorbance
dilution ratio
E)
Δ Absorbance
Concentration of CTX-AB5 (μg/mL)
F)
Intensity (a.u.)
Raman shift (cm⁻¹)
100 ng/mL
10 ng/mL
1 ng/mL
100 pg/mL
10 pg/mL
1 pg/mL
0 pg/mL
Bare chip